

This work was written as part of one of the author's official duties as an Employee of the United States Government and is therefore a work of the United States Government. In accordance with 17 U.S.C. 105, no copyright protection is available for such works under U.S. Law. Access to this work was provided by the University of Maryland, Baltimore County (UMBC) ScholarWorks@UMBC digital repository on the Maryland Shared Open Access (MD-SOAR) platform.

Please provide feedback

Please support the ScholarWorks@UMBC repository by emailing scholarworks-group@umbc.edu and telling us what having access to this work means to you and why it's important to you. Thank you.

MILLIARCSECOND STRUCTURE OF MICROARCSECOND SOURCES: COMPARISON OF SCINTILLATING AND NONSCINTILLATING EXTRAGALACTIC RADIO SOURCES

ROOPESH OJHA

Australia Telescope National Facility, Commonwealth Science and Industrial Research Organization, P.O. Box 76,
Epping, NSW 1710, Australia; roopesh.ojha@csiro.au

ALAN L. FEY

US Naval Observatory, 3450 Massachusetts Avenue NW, Washington, DC 20392-5420; afey@usno.navy.mil

DAVID L. JAUNCEY AND JAMES E. J. LOVELL

Australia Telescope National Facility, Commonwealth Science and Industrial Research Organization, P. O. Box 76,
Epping, NSW 1710, Australia; and Research School of Astronomy and Astrophysics, Mount Stromlo Observatory,
Cotter Road, Weston, ACT 2611, Australia; david.jauncey@csiro.au, jim.lovell@csiro.au

AND

KENNETH J. JOHNSTON

US Naval Observatory, 3450 Massachusetts Avenue NW, Washington, DC 20392-5420; kjj@astro.usno.navy.mil
Received 2004 March 27; accepted 2004 June 29

ABSTRACT

We compare the milliarcsecond-scale morphology of scintillating and nonscintillating sources. The scintillating sources are drawn from those flat-spectrum extragalactic radio sources discovered, by the Micro-Arcsecond Scintillation-Induced Variability Survey, to have flux density variability at 5 GHz on timescales from hours to days. Intrinsic source structure information is obtained from previously published and/or publicly available 8.4 GHz Very Long Baseline Array images. A sample of low flux density ($S_{\nu=5 \text{ GHz}} < 0.3 \text{ Jy}$) scintillating sources was compared with a sample of high flux density ($S_{\nu=5 \text{ GHz}} \sim 1 \text{ Jy}$) scintillators, as well as a sample of high flux density nonscintillators. All source samples meet the selection criteria of the Micro-Arcsecond Scintillation-Induced Variability Survey, thus ensuring that all three source samples are suitable for comparative study. We find that all scintillating sources (both low and high flux density samples) are significantly more core dominated than nonscintillating sources. Further, the overall source size of the scintillating sources is significantly smaller than that of nonscintillators. There does not appear to be any significant difference between the milliarcsecond-scale morphologies of low and high flux density scintillators. These results demonstrate that it is the core of the radio source that is scintillating.

Subject headings: galaxies: active — galaxies: ISM — galaxies: jets — galaxies: nuclei — ISM: structure — quasars: general

1. INTRODUCTION

Since the first unambiguous detection of radio variability in an extragalactic source by Dent (1965), measurement of variability has been a powerful tool for the investigation of the physics of active galactic nuclei (AGNs; e.g., Kellerman & Pauliny-Toth 1968, 1981). Notably, in the light of the discovery of radio variability on month to year timescales, causality arguments limited the physical size of sources and implied brightness temperatures that violated the inverse Compton limit (Kellerman & Pauliny-Toth 1969). This led to the adoption of bulk relativistic motion (Rees 1966) as the standard picture for AGNs, particularly after a key prediction, superluminal motion, was detected (Whitney et al. 1971; Cohen et al. 1971).

The discovery of short-term variability in some compact, flat-spectrum radio sources at centimeter wavelengths (Heeschen 1984; Heeschen et al. 1987), a phenomenon soon named intraday variability (IDV; Wagner & Witzel 1995 and references therein), pushed implied brightness temperatures as high as 10^{21} K in extreme cases (Kedziora-Chudczer et al. 1997), if the variations were assumed to be intrinsic. This would either imply Doppler factors far higher than observed (Zensus et al. 2002; Homan et al. 2001; Jorstad et al. 2001), invoke reconnection of

magnetic field lines and coherent radiation mechanisms (Benford 1992; Lesch & Pohl 1992), or require special geometric effects (Gopal-Krishna & Wiita 1992; Camenzind & Krockenberger 1992; Qian et al. 1991). As an alternative to these rather extreme conditions required by intrinsic scenarios, interstellar scintillation (ISS) was suggested as a possible explanation for IDV (Heeschen 1984; Heeschen & Rickett 1987).

While many questions remain (Krichbaum et al. 2002; Jauncey et al. 2001), it is now clear that ISS (Rickett 1990) is the principal cause of the observed centimeter-wavelength IDV in some compact, flat-spectrum radio sources. Two lines of evidence point to this conclusion. One predicted effect of ISS is a time delay in the variability pattern arrival times at two widely separated telescopes. Such time delays of minutes have been discovered for several of the most rapidly variable sources (Jauncey et al. 2000; Dennett-Thorpe & de Bruyn 2002; Bignall et al. 2002). In addition, an annual cycle in the characteristic timescale of the variability has now been found in at least five sources (Rickett et al. 2001; Jauncey & Macquart 2001; Dennett-Thorpe & de Bruyn 2001; Bignall et al. 2003; Jauncey et al. 2003). Such an annual cycle results from the changing relative velocity of the interstellar medium (ISM) seen from Earth as it moves around the Sun. For such observations, ISS is the only plausible explanation.

The Micro-Arcsecond Scintillation-Induced Variability (MASIV) Survey (Lovell et al. 2003) is a large variability survey of the northern sky using the Very Large Array (VLA) at 5 GHz. It aims to construct a sample of 100–150 scintillating extragalactic sources with which to examine both the microarcsecond structure and the parent population of these sources, as well as to probe the turbulent ISM responsible for the scintillation. From a total of 710 compact, flat-spectrum sources surveyed, over 100 new scintillating radio sources, with variability timescales from hours to days, have already been discovered by this program. One interesting result from the MASIV Survey is that there is an increase in the fraction of highly variable scintillators (those with rms flux density variations above 4%) with decreasing flux density. There is also an increase in their fractional amplitude of variability with decreasing flux density. These results raised the possibility that the milliarcsecond-scale structures of scintillators may differ from those of nonscintillators in the sense that the weaker sources are more “core dominated,” or rather, less milliarcsecond “jet” dominated.

In this paper we present a comparative study of the milliarcsecond-scale structure of three well-defined and uniformly selected samples of scintillating and nonscintillating extragalactic radio sources. Our intention is to address the following two questions: (1) Are there any morphological differences, at milliarcsecond scales, between scintillating and nonscintillating sources? (2) Are there any morphological differences, at milliarcsecond scales, between low and high flux density scintillating sources?

We describe the three groups of sources studied, including their selection criteria, in § 2. The analytical tools used and what they reveal are detailed in § 3. Our results are discussed in § 4, and § 5 gives our conclusions from this study.

2. THE DATA

For purposes of comparison we define three uniformly selected samples of scintillating and nonscintillating extragalactic radio sources. All three samples used in this study meet the selection criteria of the MASIV Survey in that they are point sources at all resolutions of the VLA and have a spectral index, from 1.4 to 4.9 GHz, flatter than 0.5. In addition, each sample meets flux density and flux density variability criteria as defined below.

Our first sample consists of the 75 low flux density scintillating (LFS) sources that were discovered to be scintillating by the MASIV Survey with rms flux density variations during a 72 hr period of $S_{\text{rms}} > [0.003^2 + (0.02S)^2]^{1/2}$ Jy, where S is the mean flux measured by the MASIV Survey at 4.9 GHz. These sources have a flux density less than 0.3 Jy at 4.9 GHz. Structural information for all of these sources was obtained from Ojha et al. (2004), who observed these sources at 8.4 GHz using the National Radio Astronomy Observatory¹ (NRAO) Very Long Baseline Array (VLBA).

The second sample consists of the 18 high flux density scintillating (HFS) sources also discovered to be scintillating by the MASIV Survey and with rms flux density variations during a 72 hr period of $S_{\text{rms}} > [0.003^2 + (0.02S)^2]^{1/2}$ Jy. These sources have a flux density ~ 1 Jy at 4.9 GHz. Structural information, at 8.4 GHz, for all of these sources was obtained

¹ The National Radio Astronomy Observatory is a facility of the National Science Foundation operated under cooperative agreement by Associated Universities, Inc.

TABLE 1
HIGH FLUX DENSITY SCINTILLATORS

Source (B1950.0)	Flux Density (Jy)	Epoch
0059+581	1.42	2002 Jan 16
0235+164	1.16	2002 Jan 16
0716+714	0.21	1997 Jan 11
0722+145	0.46	1997 Jan 10
0754+100	1.32	1997 Jan 10
0804+499	0.58	2002 Jan 16
0912+029	0.50	1997 Jan 11
0955+476	1.45	2002 Jan 16
1012+232	0.55	1998 Apr 15
1156+295	2.81	2002 Jan 16
1642+690	0.88	2002 Jan 16
1732+389	0.59	1997 Jan 11
1745+624	0.61	2002 Jan 16
1746+470	0.46	1998 Aug 10
1800+440	0.81	1997 Jan 11
2121+053	0.55	1995 Oct 02
2229+695	0.24	1997 Jan 10
2344+092	1.04	2002 Jan 16

from the US Naval Observatory (USNO) Radio Reference Frame Image Database² (RRFID). The USNO has an ongoing program to image radio reference frame sources using the VLBA. The goal of this program is to establish a database of images for all of the radio reference frame sources at the same wavelengths as those used for precise astrometry. These data allow the monitoring of sources for variability or structural changes so they can be evaluated for continued suitability as radio reference frame objects (see Fey & Charlot 2000 and references therein). Eighteen of the high flux density scintillators discovered in the MASIV program had been independently observed by this USNO program. The RRFID also contained data for a large number of the sources that the MASIV Survey found to be nonscintillators. Source names and the epoch of observation (most recent available in every case) used for this analysis are listed in Table 1. The modest size of the HFS sample must be noted, and the discovery of more sources by the MASIV Survey is eagerly anticipated.

The third sample of 144 high flux density nonscintillating (HFN) sources contains all of those objects for which no scintillating behavior was detected by the MASIV Survey and for which VLBA observations at 8.4 GHz were available in the RRFID. The flux density distribution of this sample is comparable to that of the HFS sources and distinct from that of the LFS sample. Source names and the epoch of observation (most recent available in every case) used for this analysis are listed in Table 2.

The distribution of source flux density for all three source samples is shown in Figure 1. Total flux density is defined as the total CLEANed flux density (i.e., the sum of all CLEAN components). For details of the imaging process, including CLEANing, see Ojha et al. (2004) for the LFS sources and Fey & Charlot (2000) for the HFS and HFN sources. The LFS sources have a mean flux density of 0.12 Jy with a median of 0.11 Jy. The HFS (HFN) sample has a mean flux density of 0.87 (1.13) with a median of 0.60 (0.72). Thus, the two high flux density source samples are comparable in their flux

² Available at <http://www.usno.navy.mil/RRFID>.

TABLE 2
HIGH FLUX DENSITY NONSCINTILLATORS

Source (B1950.0)	Flux Density (Jy)	Epoch
0003+380	0.54	1998 Jun 24
0007+171	0.65	1998 Aug 10
0014+813	0.66	2002 Jan 16
0016+731	1.08	1995 Oct 12
0035+413	0.45	1998 Feb 09
0039+230	0.46	1997 Jan 11
0055+300	0.64	1998 Dec 21
0106+013	1.04	1997 Jan 11
0108+388	0.87	1995 Apr 12
0111+021	0.46	1998 Aug 10
0119+041	0.57	2002 Jan 16
0119+115	1.21	2002 Jan 16
0123+257	0.54	1998 Jun 24
0133+476	2.86	2002 Jan 16
0146+056	1.13	1998 Jun 24
0148+274	0.43	1997 Jan 11
0149+218	0.82	1997 Jan 10
0201+113	0.70	2002 Jan 16
0202+149	1.74	2002 Jan 16
0212+735	3.32	1994 Jul 08
0215+015	1.35	1995 Oct 12
0221+067	0.44	1998 Aug 10
0224+671	1.17	1997 Jan 10
0234+285	3.01	2002 Jan 16
0237+040	0.69	1995 Oct 12
0239+108	1.02	1997 Jan 11
0248+430	0.87	1998 Dec 21
0300+470	0.73	1998 Jun 24
0306+102	0.48	1997 Jan 11
0309+411	0.35	1997 Jan 10
0342+147	0.27	2002 Jan 16
0400+258	0.74	1995 Apr 12
0420+417	0.65	1997 Jan 10
0440+345	0.74	1995 Apr 12
0444+634	0.87	1998 Feb 09
0446+112	0.54	1997 Jan 11
0454+844	0.22	1997 Jan 10
0457+024	0.62	2002 Jan 16
0459+060	0.68	1995 Apr 12
0500+019	0.99	1997 Jan 10
0502+049	0.55	1997 Jan 11
0507+179	0.66	1995 Apr 12
0529+075	1.19	1997 Jan 11
0536+145	1.00	1998 Dec 21
0552+398	4.33	2002 Jan 16
0609+607	0.57	1995 Oct 12
0615+820	0.42	1997 Jan 10
0636+680	0.37	1995 Apr 12
0642+449	3.04	2002 Jan 16
0650+371	0.40	1997 Jan 11
0657+172	0.84	1995 Oct 12
0707+476	0.44	1998 Aug 10
0710+439	1.12	1994 Jul 08
0735+178	0.63	1997 Jan 10
0736+017	1.29	1997 Jan 11
0738+313	2.12	1997 Jan 10
0742+103	2.00	1998 Dec 21
0745+241	0.39	1997 Jan 10
0749+540	1.01	1995 Oct 02
0805+410	0.69	1997 Jan 10
0808+019	1.10	1995 Apr 12
0812+367	0.68	1997 Jan 11
0814+425	0.93	1997 Jan 10
0820+560	0.87	1995 Oct 12

TABLE 2—Continued

Source (B1950.0)	Flux Density (Jy)	Epoch
0823+033	0.72	2002 Jan 16
0827+243	0.93	2002 Jan 16
0829+046	0.74	1997 Jan 10
0839+187	0.52	1998 Aug 10
0850+581	0.53	1997 Jan 10
0851+202	2.11	2002 Jan 16
0906+015	0.26	1997 Jan 10
0917+449	0.81	1997 Jan 10
0917+624	1.58	1995 Apr 12
0923+392	8.01	2002 Jan 16
0945+408	1.43	1995 Oct 12
0953+254	1.11	1997 Dec 17
0954+658	0.45	1997 Jan 10
1011+250	0.67	1997 Jan 11
1020+400	1.05	1995 Oct 12
1022+194	0.54	1998 Dec 21
1039+811	0.57	1997 Jan 11
1044+719	1.10	2002 Jan 16
1049+215	0.68	2002 Jan 16
1053+704	0.38	1997 Jan 11
1055+018	1.88	1998 Aug 10
1101+384	0.30	2002 Jan 16
1123+264	0.56	1997 Jan 10
1128+385	0.91	2002 Jan 16
1147+245	0.43	1997 Jan 11
1150+812	1.30	1995 Apr 12
1155+251	0.29	1997 Jan 10
1216+487	0.45	2002 Jan 16
1219+044	1.39	1998 Jun 24
1219+285	0.32	1997 Jan 10
1222+037	0.66	1997 Jan 11
1226+373	0.29	1995 Oct 12
1252+119	0.41	1997 Jan 10
1300+580	0.29	1998 Feb 09
1307+121	0.66	1995 Apr 12
1308+326	1.31	2002 Jan 16
1324+224	1.12	1997 Jan 10
1347+539	0.39	2002 Jan 16
1402+044	0.68	1998 Jun 24
1404+286	1.51	2002 Jan 16
1418+546	0.52	1998 Jun 24
1432+200	0.39	1995 Apr 12
1435+638	0.72	1997 Jan 11
1459+480	0.30	1998 Feb 09
1502+036	0.51	1997 Jan 10
1502+106	0.98	1998 Feb 09
1504+377	0.74	1997 Jan 11
1514+197	0.28	1997 Jan 10
1532+016	0.49	1998 Jun 24
1546+027	1.22	1995 Apr 12
1547+507	0.77	1998 Jun 24
1548+056	2.15	1997 Jan 11
1555+001	0.56	1997 Jan 10
1600+335	1.31	1995 Oct 12
1606+106	2.57	2002 Jan 16
1611+343	3.49	2002 Jan 16
1614+051	0.54	1997 Jan 11
1616+063	0.29	1997 Jan 10
1624+416	0.77	1995 Oct 12
1633+382	1.97	1995 Apr 12
1637+574	0.59	1997 Jan 11
1638+398	0.57	2002 Jan 16
1641+399	5.53	1998 Apr 15
1652+398	0.89	1998 Jun 24
1655+077	1.25	1997 Jan 10

TABLE 2—Continued

Source (B1950.0)	Flux Density (Jy)	Epoch
1656+053	0.59	1997 Jan 11
1656+477	0.82	1997 Jan 11
1717+178	0.54	1997 Jan 11
1725+044	0.68	1995 Apr 12
1726+455	0.76	1998 Apr 15
1727+502	0.13	1997 Jan 11
1738+476	0.56	1998 Aug 10
1739+522	0.49	2002 Jan 16
1743+173	0.82	1995 Apr 12
1749+096	3.17	2002 Jan 16
1749+701	0.44	1997 Jan 11
1751+441	0.34	1997 Jan 10
1803+784	1.91	2002 Jan 16
1807+698	0.78	1997 Jan 10
1821+107	0.49	2002 Jan 16
1823+568	1.64	1995 Oct 12
1826+796	0.54	1994 Jul 08
1842+681	0.40	1998 Feb 09
1849+670	0.86	1995 Apr 12
1856+736	0.44	1997 Jan 11
1923+210	0.59	1997 Jan 11
1947+079	0.76	1995 Apr 12
1951+355	0.34	1995 Oct 12
1954+513	1.28	1995 Apr 12
2005+403	2.05	1997 Jan 10
2007+777	1.55	1995 Oct 12
2021+614	3.13	1994 Jul 08
2023+336	2.84	1995 Oct 12
2030+547	0.48	1997 Jan 11
2037+511	2.56	1998 Apr 15
2048+312	0.41	1997 Jan 11
2059+034	0.91	1995 Oct 12
2113+293	0.98	1995 Apr 12
2134+004	7.92	1994 Jul 08
2136+141	1.97	2002 Jan 16
2144+092	0.58	1997 Jan 11
2145+067	6.09	2002 Jan 16
2149+056	0.56	1998 Apr 15
2150+173	0.56	1998 Feb 09
2209+236	0.98	1998 Apr 15
2234+282	1.28	2002 Jan 16
2251+158	8.37	1998 Feb 09
2320+506	1.33	1995 Oct 12
2328+107	0.64	1997 Jan 10
2337+264	0.56	1998 Apr 15

density distributions, and both have distinctly higher flux density distributions than the low flux density sample.

3. ANALYSIS

To investigate the milliarcsecond morphologies of our three samples, we used three measures: core fraction, flux-weighted radial extent, and unweighted radial extent. We define and describe each of these measures below. We also report what they reveal about the milliarcsecond-scale morphological structure of scintillators and non-scintillators. These results are summarized in Table 3. Table 4 lists the statistical significance of our findings.

3.1. Core Fraction

Even a cursory examination of the scintillating sources reveals that most are almost unresolved (19 LFS sources are, in fact, completely unresolved) or have a single compact

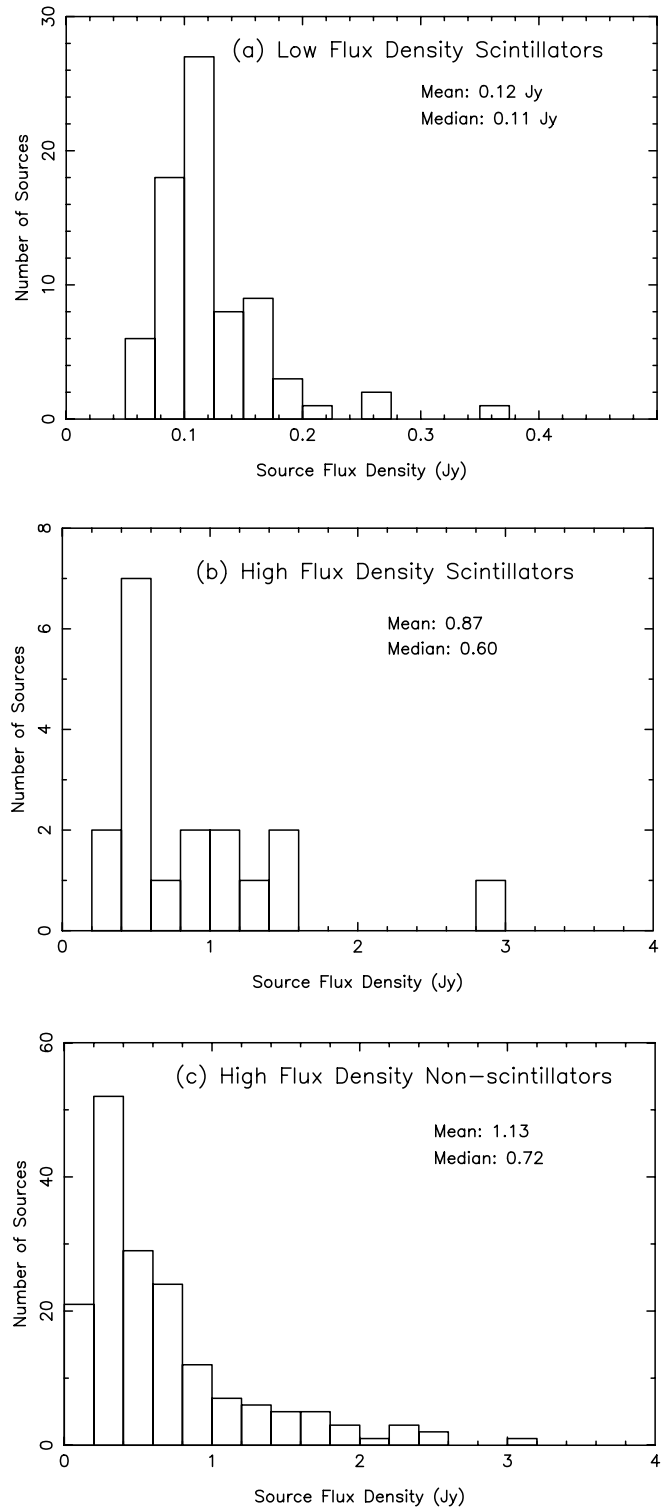


FIG. 1.—Distribution of source flux density at 8.4 GHz for the three samples of sources. Total flux density is defined as the total CLEANed flux density (i.e., the sum of all CLEAN components).

component (Ojha et al. 2004). Thus, a measure of core dominance would be a useful metric. As an estimate of the core dominance of the sources, we calculate a “core fraction” C , which is the ratio of core flux density to total flux density defined as

$$C = \frac{\sum_i (S_i)_{\text{beam}}}{\sum_i S_i}, \quad (1)$$

TABLE 3
STATISTICS OF SOURCE ANGULAR EXTENT

SAMPLE	NUMBER	C^a		R^b (mas)		$\theta_{0.95}^c$ (mas)	
		Mean	Median	Mean	Median	Mean	Median
LFS.....	75	0.90	0.94	0.29	0.16	1.62	0.83
HFS.....	18	0.86	0.91	0.29	0.22	1.59	1.04
HFN.....	174	0.73	0.76	0.76	0.52	3.36	2.07

^a Core fraction: ratio of core flux density to total flux density; see § 3.
^b Flux-weighted radial extent; see § 3.
^c Unweighted radial extent; see § 3.

where S_i is the flux density of the i th CLEAN component. In other words, core flux density is defined as the sum of the CLEANed flux density within one synthesized beam, and the total flux density is defined as the total CLEANed flux density (i.e., the sum of all CLEAN components).

The distribution of core fraction, C , for all three source samples is shown in Figure 2. The LFS and HFS sources have mean core fractions of 0.90 and 0.86 with medians of 0.94 and 0.91, respectively. A Kolmogorov-Smirnov (K-S) test (Press et al. 1992; Kolmogorov 1933; Smirnov 1936) reveals that there is a 10% chance that both of these samples are derived from the same core fraction population. This relatively low probability, when compared to that obtained by the two metrics below, probably results from the small size of the HFS sample, which lets a few outlier points affect the statistics strongly. Thus, removing just two of the four points in the 0.75–0.80 bin increases this probability to over 20%.

The nonscintillating sample, HFN, has a mean core fraction of 0.73 with a median of 0.76. On a K-S test, a common core fraction population for LFS (HFS) and HFN sources is rejected at the 99% (95%) level. Thus, both samples of scintillating sources have significantly higher core fractions than the nonscintillating sources.

3.2. Flux-weighted Radial Extent

Another, complementary, measure of core dominance is the flux density-weighted radial extent R , which is defined as

$$R = \frac{\sum_i S_i r_i}{\sum_i S_i}, \tag{2}$$

where r_i is the radius at which the i th CLEAN component has flux density S_i . Here R has units of milliarcseconds.

TABLE 4
K-S STATISTICS

SAMPLE	K-S PROBABILITY ^a		
	C^b	R^c	$\theta_{0.95}^d$
LFS-HFS.....	0.10	0.68	0.50
LFS-HFN.....	0.00	0.00	0.00
HFS-HFN.....	0.05	0.00	0.03

^a Probability that the samples belong to the same parent core fraction population.
^b Core fraction: ratio of core flux density to total flux density; see § 3.
^c Flux-weighted radial extent; see § 3.
^d Unweighted radial extent; see § 3.

The distribution of flux-weighted radial extent, R , for all three source samples is shown in Figure 3. Note that, in order to use the same scale for all three histograms, three outliers with $R > 4$ are not shown; all three belong to the HFN sample. The mean (median) values of the flux-weighted radial extent are 0.29 (0.16) and 0.29 (0.22) mas for the LFS and HFS sources, respectively. This is in sharp contrast with a mean (median) of 0.76 (0.52) for the HFN sample. A K-S test rejects a common parent population for LFS (HFS) and HFN sources at the 99% (99%) level. On the other hand, the LFS and HFS samples have a 68% probability of being derived from a common core fraction population.

Thus, this study of flux-weighted radial extent confirms the above result that both samples of scintillating sources are significantly more core dominant than the nonscintillators. Furthermore, the LFS and HFS samples are consistent with the same parent core fraction population.

3.3. Unweighted Radial Extent

As a straightforward measure of overall source size, i.e., the maximum radial extent of the source, we calculate a quantity E , similar to C above, as

$$E = \frac{\sum_i (S_i)_{\theta}}{\sum_i S_i}, \tag{3}$$

where the numerator now represents the flux density contained within an area of angular radius $0 \leq \theta < \infty$. The maximum radial extent of the source, $\theta_{0.95}$, is then defined as the value of θ when $E \geq 0.95$, i.e., when the area of angular radius θ contains 95% of the total CLEANed flux density. Here $\theta_{0.95}$ has units of milliarcseconds.

The distribution of unweighted radial extent, $\theta_{0.95}$, for all three source samples is shown in Figure 4. Note that, in order to use the same scale for all three histograms, outliers with $\theta_{0.95} > 15$ are not shown. There are one, zero, and five such outliers in the LFS, HFS, and HFN samples, respectively. The mean (median) values of the unweighted radial extent are 1.62 (0.83) and 1.59 (1.04) mas for the LFS and HFS sources, respectively. Once again, this is in sharp contrast with a mean (median) of 3.36 (2.07) for the HFN sample. A K-S test rejects a common parent population for LFS (HFS) and HFN sources at the 99% (97%) level. The LFS and HFS samples have a 50% probability of being derived from a common parent core fraction population.

Thus, similar to the situation for core dominance, both the low and high flux density scintillator samples have significantly less overall source extent than the nonscintillator sample. In addition, the distributions of overall source extent for the two

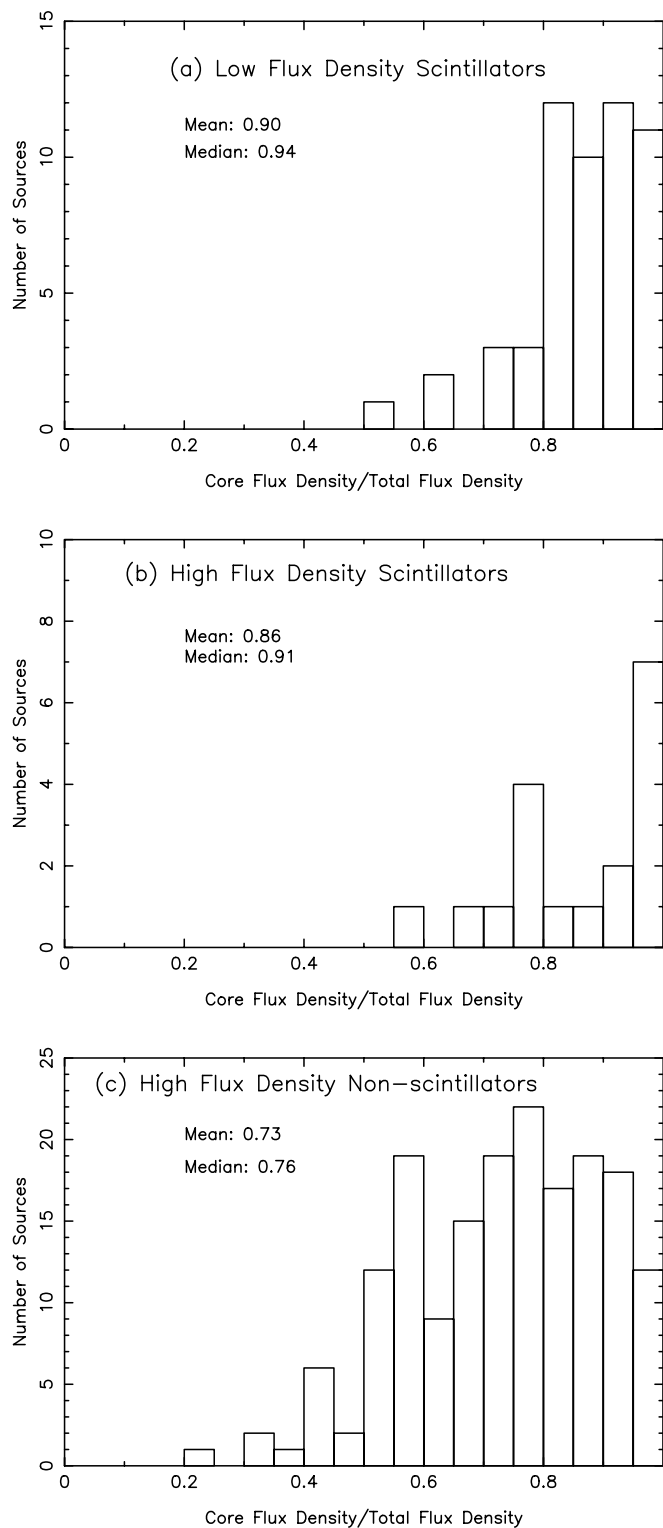


FIG. 2.—Distribution of source core fraction (ratio of core flux density to total flux density) at 8.4 GHz for the three samples of sources. Core flux density is defined as the sum of the CLEANed flux density within one synthesized beam. The total flux density is defined as the total CLEANed flux density (i.e., the sum of all CLEAN components).

scintillating samples are consistent with the same parent, core fraction population.

4. DISCUSSION

It has long been suggested (e.g., Quirrenbach et al. 1992) that the occurrence of IDV may be correlated with the

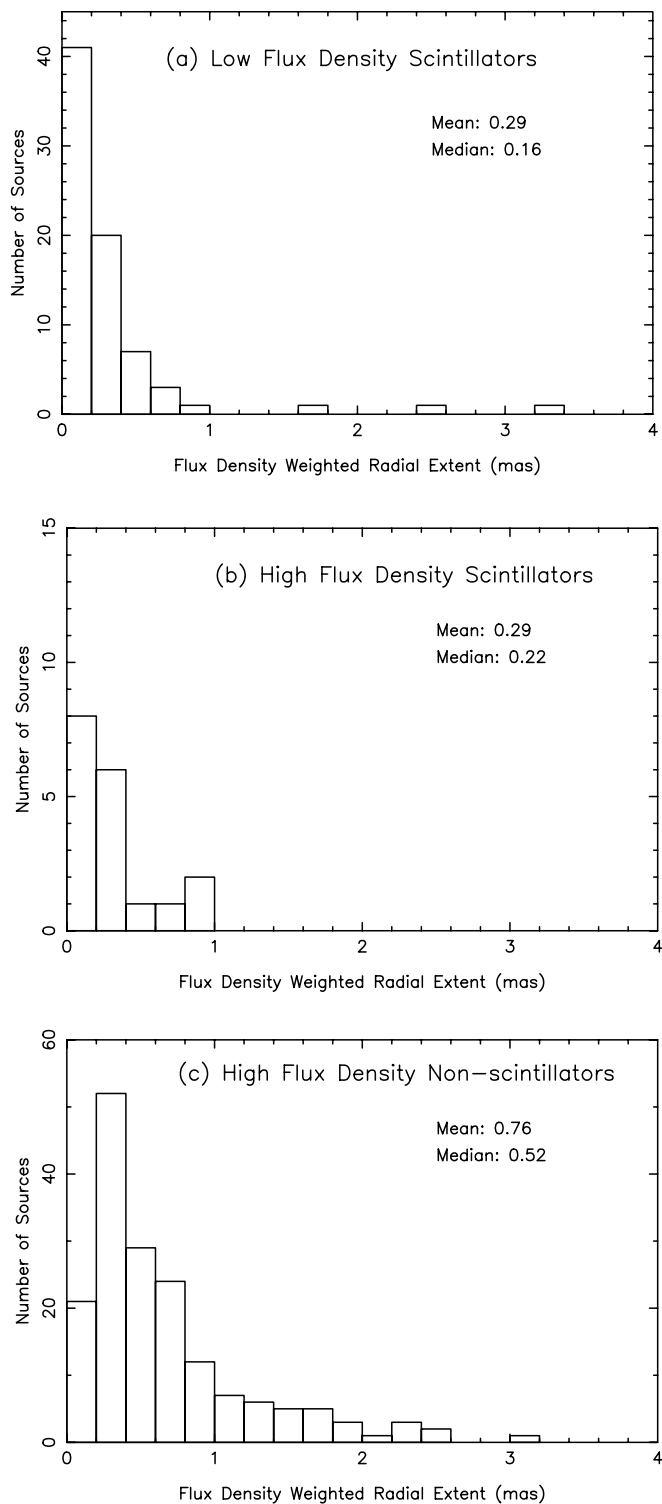


FIG. 3.—Distribution of 8.4 GHz flux density-weighted radial extent for the three samples of sources.

milliarcsecond-scale structure of AGNs, being common in core-dominated objects and rare in objects with a bright VLBI scale jet. The MASIV Survey found that the fraction of scintillating sources increases strongly with decreasing flux density. This may result from the microarcsecond scintillating components being brightness temperature limited, as might be expected from an inverse Compton-limited brightness temperature. Alternatively, it may be the result of sampling a different source population among the weaker sources, in

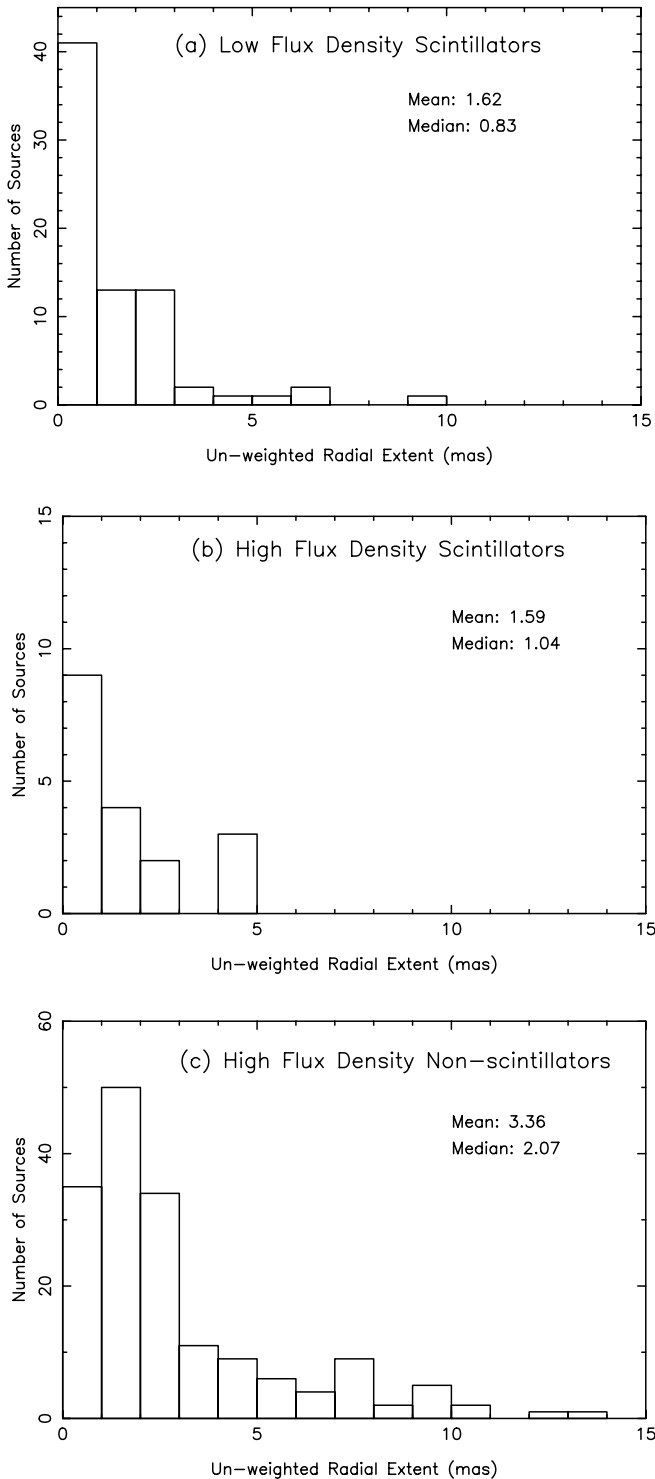


FIG. 4.—Distribution of unweighted radial extent at 8.4 GHz for the three samples of sources.

the sense that the weaker sources are more “core dominated,” or rather, less milliarcsecond “jet” dominated. Thus, the MASIV Survey underscored the possibility that the LFS sources may form a population with distinct milliarcsecond-scale morphology.

Ojha et al. (2004) used the VLBA to conduct the first large-scale survey of the milliarcsecond structure of 75 LFS sources at 8.4 GHz. The RRFID had independently imaged most of the HFS sources and a large number of HFN sources at 8.4 GHz

with the VLBA. By selecting all three samples using the MASIV criteria, we obtained three well-defined samples that can be meaningfully compared. However, two caveats are in order. First, the sample of HFS sources is limited by the number discovered that meet the MASIV selection criteria and is relatively small. However, this 18-source sample is large enough for the K-S test to be valid.³ Second, comparison of the LFS sources with HFN sources should be treated with caution as sensitivity limits could bias the results in the sense that weak extended structure in the LFS sample might not be detected.

The milliarcsecond-scale morphology of the LFS, HFS, and HFN samples was characterized in a number of ways detailed in § 3, primarily in order to address two questions: (1) Are there any morphological differences, at milliarcsecond scales, between scintillating and nonscintillating sources? (2) Are there any morphological differences, at milliarcsecond scales, between low and high flux density scintillating sources? Bearing the above-mentioned caveats in mind, we appear to have a clear answer to both questions.

Yes, there are significant differences between the milliarcsecond-scale morphology of scintillating and nonscintillating sources. Both the low and high flux density scintillator samples have significantly higher “core fraction” and significantly smaller “flux-weighted linear extent” than the nonscintillator sample. Both these metrics of core dominance clearly lead to the conclusion that scintillating sources are significantly more core dominant than nonscintillating sources. Further, the overall angular size distribution, as determined by the “unweighted linear extent” metric, indicates that both low and high flux density scintillating sources have significantly smaller angular size than nonscintillators.

No, there are no significant differences between the milliarcsecond-scale morphology of low and high flux density scintillators. All metrics suggest that LFS and HFS samples are consistent with the same parent core fraction population.

These results strongly support the model that it is the cores of the extragalactic sources that scintillate in the ISM, not the bright milliarcsecond jets.

An exhaustive exploration of the flux density–modulation index parameter space would require a fourth sample of low flux density nonscintillator (LFN) sources. Such a sample is not currently available and will be included in future work. However, given that there do not appear to be any significant differences between low and high flux density scintillators, we have grounds to expect that the milliarcsecond morphology of low flux density nonscintillators might be similar to that of their high flux density counterparts (and different from that of all scintillating sources).

5. CONCLUSIONS

We have analyzed the milliarcsecond-scale morphology of the first large and well-defined samples of low and high flux density scintillators, as well as high flux density non-scintillators. Our analysis shows that both low and high flux density scintillators have significantly different morphologies than nonscintillators. On average, scintillating sources have a higher proportion of their flux in a compact core. Scintillating sources also have a smaller overall angular size. Low

³ The K-S test becomes asymptotically accurate as the effective number of data points, $N_e = N_1 N_2 / (N_1 + N_2)$, becomes large, but it is already good for $N_e \geq 4$. Even for the smaller two of our samples, $N_e = 14.5$. Note that N_1 and N_2 are the number of data points in the first and second distributions, respectively.

and high flux density scintillators do not, on average, have different morphologies. Thus, our results support the paradigm that scintillation originates in the cores of AGNs and its observed magnitude is diminished in the presence of a bright milliarcsecond-scale jet.

To complete the exploration of the flux density–modulation index parameter space, observations of a fourth sample, that of LFN sources, are planned. As there do not appear to be any significant differences between low and high flux density scintillators, we predict that the milliarcsecond-scale morphologies of low flux density nonscintillators are likely to be

similar to their high flux density counterparts and different from those of all scintillating sources.

We thank Hayley E. Bignall, Lucyna Kedziora-Chudczer, and Jean-Paul Macquart for useful discussions. R. O. dedicates this paper to Dr. G. P. Ojha. This research has made use of the US Naval Observatory (USNO) Radio Reference Frame Image Database (RRFID) and NASA's Astrophysics Data System Abstract Service. Facilities: VLBA, VLA.

REFERENCES

- Benford, G. 1992, *ApJ*, 391, L59
 Bignall, H. E., et al. 2002, *Publ. Astron. Soc. Australia*, 19, 29
 ———. 2003, *ApJ*, 585, 653
 Camenzind, M., & Krockenberger, M. 1992, *A&A*, 255, 59
 Cohen, M. H., Cannon, W., Purcell, G. H., Shaffer, D. B., Broderick, J. J., Kellermann, K. I., & Jauncey, D. L. 1971, *ApJ*, 170, 207
 Dennett-Thorpe, J., & de Bruyn, A. G. 2001, *Ap&SS*, 278, 101
 ———. 2002, *Nature*, 415, 57
 Dent, W. A. 1965, *Science*, 148, 1458
 Fey, A. L., & Charlot, P. 2000, *ApJS*, 128, 17
 Gopal-Krishna, & Wiita, P. J. 1992, *A&A*, 259, 109
 Heesch, D. S. 1984, *AJ*, 89, 1111
 Heesch, D. S., Krichbaum, T. P., Schalinski, C. J., & Witzel, A. 1987, *AJ*, 94, 1493
 Heesch, D. S., & Rickett, B. J. 1987, *AJ*, 93, 589
 Homan, D. C., Ojha, R., Wardle, J. F. C., Roberts, D. H., Aller, M. F., Aller, H. D., & Hughes, P. A. 2001, *ApJ*, 549, 840
 Jauncey, D. L., Johnston, H. M., Bignall, H. E., Lovell, J. E. J., Kedziora-Chudczer, L., Tzioumis, A. K., & Macquart, J.-P. 2003, *Ap&SS*, 288, 63
 Jauncey, D. L., Kedziora-Chudczer, L. L., Lovell, J. E. J., Nicholson, G. D., Perley, R. A., Reynolds, J. E., Tzioumis, A. K., & Wieringa, M. H. 2000, in *Astrophysical Phenomena Revealed by Space VLBI*, ed. H. Hirabayashi, P. G. Edwards, & D. W. Murphy (Kanagawa: ISAS), 147
 Jauncey, D. L., & Macquart, J.-P. 2001, *A&A*, 370, L9
 Jauncey, D. L., et al. 2001, *Ap&SS*, 278, 87
 Jorstad, S. G., Marscher, A. P., Mattox, J. R., Wehrle, A. E., Bloom, S. D., & Yurchenko, A. V. 2001, *ApJS*, 134, 181
 Kedziora-Chudczer, L., Jauncey, D. L., Wieringa, M. H., Walker, M. A., Nicolson, G. D., Reynolds, J. E., & Tzioumis, A. K. 1997, *ApJ*, 490, L9
 Kellerman, K. I., & Pauliny-Toth, I. I. K. 1968, *ARA&A*, 6, 417
 ———. 1969, *ApJ*, 155, L71
 ———. 1981, *ARA&A*, 19, 373
 Kolmogorov, A. 1933, *G. Ist. Attuari*, 4, 83
 Krichbaum, T. P., Kraus, A., Fuhrmann, L., Cimò, G., & Witzel, A. 2002, *Publ. Astron. Soc. Australia*, 19, 14
 Lesch, H., & Pöhl, M. 1992, *A&A*, 254, 29
 Lovell, J. E. J., Jauncey, D. L., Bignall, H. E., Kedziora-Chudczer, L., Macquart, J.-P., Rickett, B. J., & Tzioumis, A. K. 2003, *AJ*, 126, 1699
 Ojha, R., Fey, A. L., Lovell, J. E. J., Jauncey, D. L., & Johnston, K. J. 2004, *AJ*, in press
 Press, W. H., Teukolsky, S. A., Vetterling, W. T., & Flannery, B. P. 1992, *Numerical Recipes in C: The Art of Scientific Computing* (Cambridge: Cambridge Univ. Press)
 Qian, S. J., Quirrenbach, A., Witzel, A., Krichbaum, T. P., Hummel, C. A., & Zensus, J. A. 1991, *A&A*, 241, 15
 Quirrenbach, A., et al. 1992, *A&A*, 258, 279
 Rees, M. J. 1966, *Nature*, 211, 468
 Rickett, B. J. 1990, *ARA&A*, 28, 561
 Rickett, B. J., Witzel, A., Kraus, A., Krichbaum, T. P., & Qian, S. J. 2001, *ApJ*, 550, L11
 Smirnov, N. V. 1936, *CR Acad. Sci. Paris*, 202, 449
 Wagner, S. J., & Witzel, A. 1995, *ARA&A*, 33, 163
 Whitney, A. R., et al. 1971, *Science*, 173, 225
 Zensus, J. A., Ros, E., Kellermann, K. I., Cohen, M. H., Vermeulen, R. C., & Kadler, M. 2002, *AJ*, 124, 662